On the magnetic structure of $(Fe_{1-x}Mn_x)Pt$: A first-principles study

Hu-Bin Luo [a,b,*], Wei-Xing Xia [a,b], Juan Du [a,b], Jian Zhang [a,b], J. Ping Liu [c], Aru Yan [a,b]

[a] Key Laboratory of Magnetic Materials and Devices, Ningbo Institute of Material Technology and Engineering, Chinese Academy of Sciences, Ningbo 315201, People's Republic of China
[b] Zhejiang Province Key Laboratory of Magnetic Materials and Application Technology, Ningbo Institute of Material Technology and Engineering, Chinese Academy of Sciences, Ningbo 315201, People's Republic of China
[c] Department of Physics, University of Texas at Arlington, Arlington, TX 76091, USA

ARTICLE INFO

Keywords:
Magnetic recording
Magnetic structure
Phase stability
Exchange interaction

ABSTRACT

This study investigates the composition dependence of magnetic structures of $(Fe_{1-x}Mn_x)Pt$ using first-principles method. A series of possible magnetic configurations are considered in the calculation to compare the relative stabilities after structural optimization, based on which, together with the comparison between theoretical and experimental magnetic properties, the results largely support the experimental finding in powders. The experimentally found stability of ferrimagnetic state in films with a wide composition range of $x \leq 0.5$ is not fully supported by this study. The composition-dependent magnetic structures are discussed according to the exchange interactions.

1. Introduction

As a promising material for ultrahigh-density magnetic storage, FePt has attracted much attention in recent years, about which the research interest covers preparation and characterization of nanostructures, order–disorder transition and magnetic properties [1–6]. In addition, many research efforts have been dedicated to the investigation of its ternary or quaternary compounds in order to tune the saturation magnetization (M_S) and magnetocrystalline anisotropy (K_U), Curie temperature, ordering kinetics and so on [7–13]. For instance, both the M_S and K_U of thin-film FePt were found to decrease steadily when Fe site was doped by Ni, Co, and Cr, from which the relationship between M_S (K_U) and the number of valence electron was generalized approximately independent of dopant species. This was further verified by the experiment of Meyer and Thiele on $(Fe_{1-x}Mn_x)Pt$ films, finding that M_S decreases to be zero at $x=0.5$ [9]. A net antiferromagnetic coupling between Fe and Mn was thus concluded (ferrimagnetic). However, earlier measurements by Menshikov et al. using neutron diffraction showed a complicated magnetic phase diagram of $(Fe_{1-x}Mn_x)Pt$ powders [14]. According to that, the composition range for ferromagnetic state is $x \leq 0.06$ at 4.2 K and $x \leq 0.2$ under room temperature. For $x > 0.2$, it is antiferromagnetic with $M_S = 0$. This does not agree with the result of steady drop of M_S with x found in the films.

Recently, Gruner and Entel investigated the stability of $(Fe_{1-x}Mn_x)Pt$ nanoparticles (561 atoms) with several magnetic configurations using first-principles plane-wave pseudopotential method in combination with magic-number clusters approach [11]. The results showed alternate stabilities of the considered configurations with changing composition. Possible new functional applications such as inverse magnetocaloric effect in the alloy are thus proposed, which may be of interest in the future. However, both the evolution of mean magnetic moments of (Fe, Mn) site defined as $\bar{\mu}_{(Fe,Mn)} = \sum_i^n (|\mu^i_{(Fe,\,Mn)}|/n)$ (n is the number of magnetic sublattice) obtained by Menshikov et al. [14] and the stability of ferrimagnetic phase found by Meyer and Thiele [9] remain not well accounted for due to the complicated magnetic phase transitions in the alloys. In that calculation, it was assumed that Fe moments aligned with the same wave vector ($\mathbf{q}$) as Mn moments in the configurations. This may not be adequate to address the complicated magnetic phases in the alloy since the ferromagnetism in FePt and antiferromagnetism in MnPt indicate the possibility that Fe and Mn moments align in different ways (different $\mathbf{q}$) in $(Fe_{1-x}Mn_x)Pt$. Besides, the flipping of Mn moments needs to be considered extensively in addition to the ferrimagnetic case.

Inspired by the above mentioned, this study has selected a series of possible magnetic structures of $(Fe_{1-x}Mn_x)Pt$ and calculated their energies within density functional theory [15]. After the analysis of energetic stabilities and the magnetic properties compared with the experimental ones, we shall see that the

* Corresponding author at: Key Laboratory of Magnetic Materials and Devices, Ningbo Institute of Material Technology and Engineering, Chinese Academy of Sciences, Ningbo 315201, People's Republic of China.
E-mail addresses: hubin.luo@gmail.com (H.-B. Luo), xiawxing@nimte.ac.cn (W.-X. Xia).

consideration of more configurations beyond those in Ref. [11] is necessary to offer important knowledge about the composition dependence of the complicated phases before exploring the functional application of $(Fe_{1-x}Mn_x)Pt$.

2. Models and calculation details

The ferromagnetic and possible antiferromagnetic configurations of interest here are shown in Fig. 1, which are taken from those reported or considered in the literatures [9,11,14,16]. They are referred to as FM, AF1, AF2 and AF3 which correspond to $\mathbf{q} = (2\pi/a)(000)$, $(2\pi/a)(10\frac{1}{2})$, $(2\pi/a)(001)$ and $(2\pi/a)(100)$, respectively, in the presentation of face centered cubic lattice (one ferromagnetic and three antiferromagnetic). For the cases with flipped Mn moments, i.e., Fe and Mn moments align antiparallelly on the same sublattice, we refer to them as $FM^{\uparrow}-FM^{\downarrow}$ (ferrimagnetic), $AF1^{\uparrow}-AF1^{\downarrow}$, $AF2^{\uparrow}-AF2^{\downarrow}$ and $AF3^{\uparrow}-AF3^{\downarrow}$, respectively. Since the ground state of FePt is ferromagnetic and the ground state of MnPt is antiferromagnetic, three configurations are generated from the combinations of those in Fig. 1, which are referred to as FM–AF1, FM–AF2 and FM–AF3 denoting that Fe moments align ferromagnetically but Mn moments align antiferromagnetically. Similarly, AF1–AF3 is considered following the reported magnetic structure in Ref. [14]. In these four cases, the flipping of Mn moments produces no difference. Although the non-collinear states were reported in some composition regions [14], in this study, all magnetic moments are treated collinearly. This is based on several considerations: (i) the calculation is to give a qualitative picture of the magnetic structure in the alloys; (ii) the difference in exchange energy due to different magnetic alignments is usually large compared with the spin–orbit interaction that results in the non-collinear alignment; and (iii) to reduce the computational load.

Since the alloy involves random distribution of Fe and Mn atoms, it is a good choice to adopt coherent potential approximation (CPA) for the study of this kind [17,18], which also facilitates the calculation of complicated magnetic structures. The calculation technique applied herein is the first-principles exact muffin-tin orbitals (EMTO) based on an improved screened Koringa–Kohn–Rostoker method in combination with CPA [19,20]. The scalar-relativistic Green's function was adopted to solve the one-electron Kohn–Sham equation. The one-electron potential was represented by optimized overlapping muffin-tin potential spheres with soft-core approximation. The full-charge density correction was introduced in the total energy calculations [20]. The electronic exchange-correlation potential was described with the generalized gradient approximation parameterized by Perdew et al. [21]. The *spdf* orbitals were included in the EMTO basis sets to construct the wave functions. The Fe-$3d^74s^1$, Mn-$3d^54s^2$ and Pt-$5d^86s^2$ were treated as valence states. A Gaussian mesh of 16 energy points on a semicircle with 1 Ry in diameter comprising the valence states was used for energy integration. The Brillouin zone was sampled by special *k*-point technique [22] with a mesh of $17 \times 17 \times 19$ for FM, AF3 and FM–AF3, and a mesh of $17 \times 17 \times 9$ for AF1, AF2, FM–AF1 and FM–AF2. To calculate the exchange interaction, the magnetic force theorem is adopted [23].

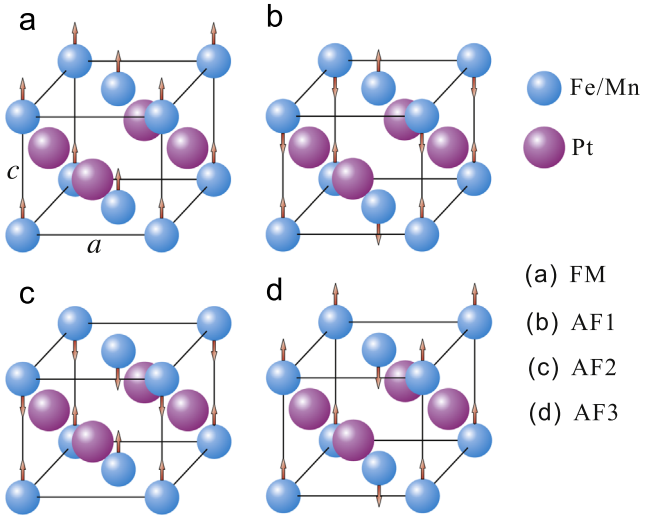

Fig. 1. Ferromagnetic and antiferromagnetic configurations for $(Fe_{1-x}Mn_x)Pt$ with wave vectors of $(2\pi/a)(000)$ (a), $(2\pi/a)(10\frac{1}{2})$ (b), $(2\pi/a)(001)$ (c) and $(2\pi/a)(100)$ (d) in the presentation of face centered cubic lattice.

3. Results and discussions

3.1. Structural properties and relative stability

The most sensitive structural parameter to magnetic configurations is the *c/a* and thus is of interest here. In Fig. 2, we show the calculated *c/a* of $(Fe_{1-x}Mn_x)Pt$ without flipped Mn moments and the available experimental results. It is found that the difference in *c/a* and its composition dependence can be significant for the alloys with different magnetic configurations. For FePt, it has the largest *c/a* for FM (0.972) and the lowest for AF3 (0.910), whereas, for MnPt, the situation is reversed with 0.925 for AF3 and 0.812 for FM. These results are very close to the recent first-principles calculation of FePt and MnPt by Lu et al. [16]. It is interesting that the *c/a* of MnPt for AF1 is quite close to that for AF3, and the composition dependence of *c/a* for FM–AF1 (AF1) is similar to that for FM–AF3 (AF1–AF3). Considering the sequence of phase transition with increasing *x*, i.e., FM → AF1 → AF3, reported by Menshikov et al. [14], the *c/a* should decrease with *x* because *c/a* deceases in this phase sequence as shown in the figure. This agrees with the measured decreasing *c/a* with *x* that varies in between the calculated ones of FM and AF3. The *c/a* reported by Meyer and Thiele shows similar composition dependence to that reported by Menshikov et al., although they were believed to belong to different magnetic phases [9,14].

The relative stabilities of magnetic configurations without flipped Mn moments are shown in Fig. 3, in which the zero energies are set as those of FM state. For FePt, although the most

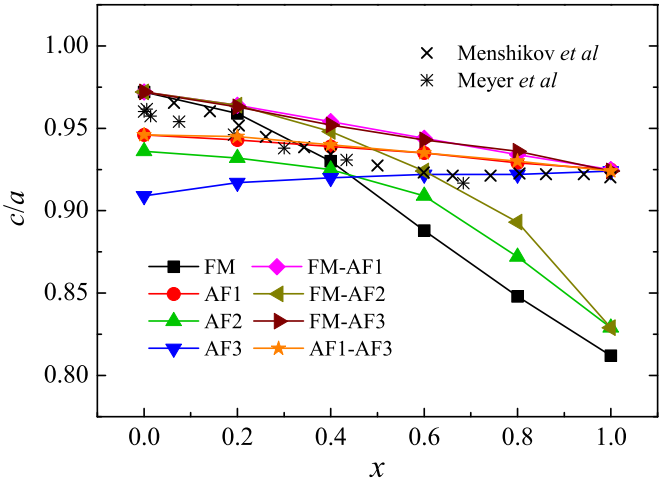

Fig. 2. The calculated *c/a* for different magnetic configurations without flipped Mn moments. The available experimental data measured in powders [14] and films [9] are also plotted for comparison.

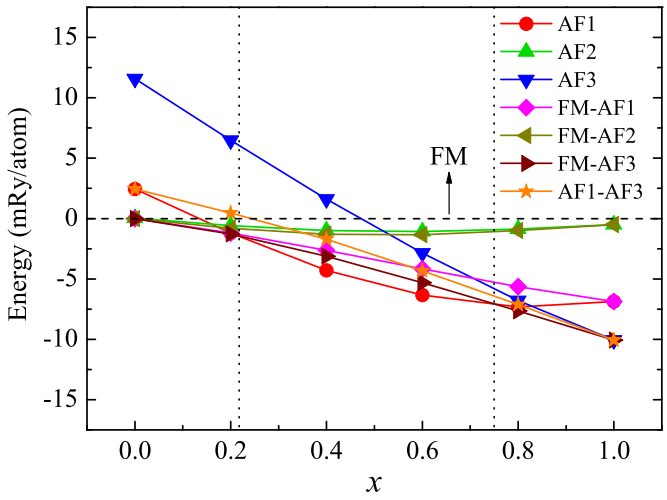

Fig. 3. The calculated energies for different magnetic configurations without flipped Mn moments. The energy of FM is chosen as the reference.

stable configuration is FM, the closeness between the energies of AF2 and FM indicates that the antiferromagnetic coupling between (001) Fe planes is significant at lower c/a (cf. Fig. 2), agreeing with the finding by Brown et al. using first-principles calculation [24]. For MnPt, AF3 has the lowest energy, consistent with the ground state widely reported in the literature [11,16]. For $x=0.2$, although FM–AF3 has the lowest energy of −1.289 mRy/atom, the energies of AF1, FM–AF1 and AF3 are very close to each other. It can be expected that the energies of FM–AF1, FM–AF2, FM–AF3 and AF2 are close to each other in the range of $x \leq 0.2$ according to the evolution of these energies with respect to x as shown in the figure. Similar relations apply also to the energies of FM–AF3, AF1–AF3 and AF3 in the range of $x \geq 0.8$. As x increases to be larger than 0.22, AF1 becomes energetically favorable. The situation alters at $x=0.75$, where FM–AF3 becomes more stable until it finally transits to AF3.

For the magnetic configurations with flipped Mn moments, in Table 1, we present their c/a's and relative energies (ΔE) to those without flipped Mn moments as presented in Fig. 3. Compared with the c/a's in Fig. 2, except for AF1$^{\uparrow}$ – AF1$^{\downarrow}$, of which the c/a remains basically unchanged, all of the cases are subjected to an increase in c/a of typically 0.01–0.02. The flipping of Mn moments results in an enhanced stability (negative ΔE) for FM$^{\uparrow}$ – FM$^{\downarrow}$ compared with FM, in contrast to the significantly reduced stability (positive ΔE) for AF1$^{\uparrow}$ – AF1$^{\downarrow}$ relative to AF1. ΔE varies from positive to negative with x for AF2$^{\uparrow}$ – AF2$^{\downarrow}$ and oscillates around zero for AF3$^{\uparrow}$ – AF3$^{\downarrow}$. However, it is noted that ΔE is small for the latter two configurations.

The calculated stabilities of the magnetic configurations can be summarized according to Fig. 3 and Table 1. For $x=0.2$, the energy of FM$^{\uparrow}$ – FM$^{\downarrow}$ (−1.285 mRy/atom) is marginally lower than those of AF1 (−1.201 mRy/atom) and FM–AF1 (−1.200 mRy/atom) and is quite close to that of FM–AF3 (−1.289 mRy/atom). For most of compositions considered, the ground states are still those determined in Fig. 3, i.e., AF1 for $0.22 < x < 0.75$ and FM–AF3 for $0.75 < x < 0.8$. However, our additional calculation for $x=0.9$ shows that the AF3$^{\uparrow}$ – AF3$^{\downarrow}$ becomes most stable, which is consistent with the result measured in powder samples [14]. It is noted that the results of FM, FM$^{\uparrow}$ – FM$^{\downarrow}$, AF1, AF2 and AF3 presented in Fig. 3 and Table 1 agree with those calculated by Gruner and Entel for ($Fe_{1-x}Mn_x$)Pt nanoparticles [11].

It is clear that FM is no longer the ground state on doping Mn, contrary to the reported stability of FM in $x < 0.06$ by Menshikov et al. [14]. The calculation does not fully reproduce the stabilized FM$^{\uparrow}$ – FM$^{\downarrow}$ in the range of $0 < x < 0.5$ found in the thin films, which may originate in the bulk calculation adopted here. The composition of $x=0.22$ at which AF1 becomes the ground state agrees very well with the results measured in powder samples, which showed that AF1 became the ground state when x was larger than 0.2 [14]. The predicted stable AF1 in the range of $0.5 < x < 0.75$ and stable FM–AF3 in the range of $0.75 < x < 0.8$ do not agree with the reported canted AF1–AF3 ($0.5 < x < 0.8$) in powder samples. However, the energies of AF1–AF3 in this range are typically more than 0.6 mRy/atom higher than those of the most stable ones (cf. Fig. 3). This energy difference is too large to be compensated even if we consider the spin–orbit coupling (reason of canting) and do non-collinear calculations. The possible reason for the discrepancy between theory and experiment may be that the calculation ideally treats the substitution of Fe by Mn as homogeneous, whereas the samples were subjected to local inhomogeneity.

Table 1
The energies (in mRy/atom) for magnetic configurations with Fe and Mn moments aligning antiparallelly on the same sublattice relative to those of magnetic configurations with Fe and Mn moments aligning in parallel (cf. Fig. 3). The corresponding c/a's are also presented.

Alloy (x)	FM$^{\uparrow}$ – FM$^{\downarrow}$		AF1$^{\uparrow}$ – AF1$^{\downarrow}$		AF2$^{\uparrow}$ – AF2$^{\downarrow}$		AF3$^{\uparrow}$ – AF3$^{\downarrow}$	
	c/a	ΔE	c/a	ΔE	c/a	ΔE	c/a	ΔE
0.2	0.961	−1.285	0.944	3.303	0.943	0.021	0.941	−0.168
0.4	0.942	−1.502	0.938	5.198	0.939	0.005	0.939	0.243
0.6	0.909	−1.021	0.933	4.782	0.926	−0.026	0.930	−0.156
0.8	0.858	−0.430	0.926	3.363	0.896	−0.125	0.926	0.153

3.2. Magnetic moments

In Fig. 4, we present the total magnetic moments per formula unit (μ_{tot}) and the mean magnetic moments per (Fe,Mn) site [$\overline{\mu}_{(Fe,Mn)}$] of all configurations considered and make comparison with the available experimental data [9,14]. For the cases with flipped Mn moments, FM$^{\uparrow}$ – FM$^{\downarrow}$ and AF3$^{\uparrow}$ – AF3$^{\downarrow}$ are considered due to their low energies at $x=0.2$ and 0.8, respectively. In the left panel, μ_{tot} of FM increases linearly with x due to the larger moment of Mn than Fe, whereas μ_{tot} of FM–(AF1/AF2/AF3) decreases linearly with x simply because of the reducing amount of Fe (Mn moments align antiferromagnetically). The kink at $x=0.45$ in the $\mu_{tot} \sim x$ of FM$^{\uparrow}$ – FM$^{\downarrow}$ indicates that, with x further increases, the overall Fe moments are surpassed by the overall antiparallel Mn

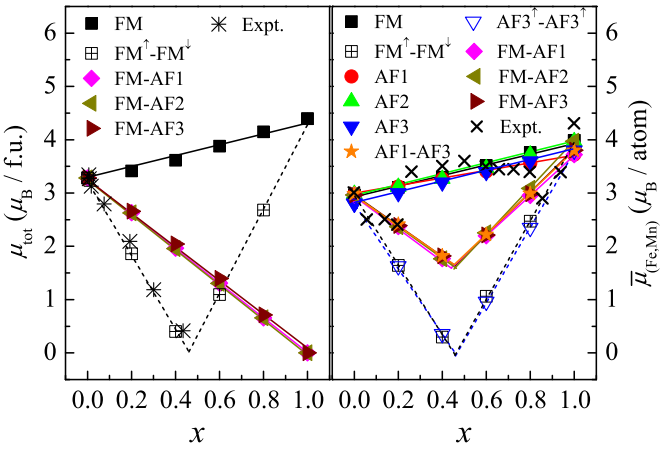

Fig. 4. The total magnetic moments per formula unit (left panel) and the mean magnetic moments per (Fe, Mn) site (right panel) for different configurations as functions of x. The total magnetic moments of antiferromagnetic states are always zero and thus are not plotted. The experimental data were measured by Meyer and Thiele (left panel) [9] and Menshikov et al. (right panel) [14], respectively.

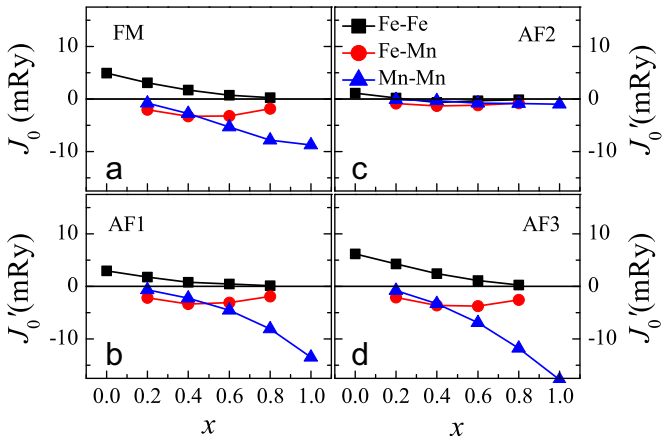

Fig. 5. The exchange interactions of FM (a), AF1 (b), AF2 (c) and AF3 (d) as functions of composition. For FM, the exchange interactions are calculated within the single (Fe, Mn) sublattice, while, for AF1, AF2 and AF3, they are those interactions between the two (Fe, Mn) sublattices (see more in the text).

moments. In the right panel, similarly, the kinks in $\overline{\mu}_{(Fe,Mn)}$ result from the existence of antiparallel alignment of Mn moments with Fe moments on the single sublattice of $FM^{\uparrow}-FM^{\downarrow}$ and on one of the sublattices in FM–(AF1/AF2/AF3) and AF1–AF3. Otherwise, $\overline{\mu}_{(Fe,Mn)}$ increases linearly with x.

It is seen that the calculated magnetic properties for FePt and MnPt are in good agreement with the experiments [9,14]. Although this study does not support a wide-range stability of $FM^{\uparrow}-FM^{\downarrow}$, it gives the corresponding μ_{tot}'s well agreeing with those measured in films. The $\overline{\mu}_{(Fe,Mn)}$ measured in powder samples drops first according to $FM^{\uparrow}-FM^{\downarrow}$ with x for $x \le 0.06$ ($AF3^{\uparrow}-AF3^{\downarrow}$ is ruled out due to its high energy) and then varies with x in accordance with FM–(AF1/AF2/AF3) in the range of $0.06 < x \le 0.2$. Considering the above discussion about the close stabilities of these configurations, this study tends to support that $FM^{\uparrow}-FM^{\downarrow}$ is stabilized in $x \le 0.06$ and mixed state is formed in $0.06 < x < 0.2$ as found in the powder samples [14]. For $0.2 < x < 0.5$, the linear increase in $\overline{\mu}_{(Fe,Mn)}$ of the stabilized AF1 with x agrees well with the experiment. For $0.5 < x < 0.8$, according to the above presented stabilities of magnetic structures, $\overline{\mu}_{(Fe,Mn)}$ should increase linearly with x until $x=0.75$ and then drop to coincide with that of FM–AF3, which differs from the gradual decrease in $\overline{\mu}_{(Fe,Mn)}$ due to (i) the failure to reproduce the experimentally found AF1–AF3 state and (ii) collinear calculation considered here. The linear increase in the $\overline{\mu}_{(Fe,Mn)}$ of the stabilized $AF3^{\uparrow}-AF3^{\downarrow}$ is also verified by the experimental ones in the range of $x > 0.86$.

3.3. Exchange interactions

The stabilities of magnetic structures may be qualitatively interpreted by the exchange interactions (J_0) in $(Fe_{1-x}Mn_x)Pt$, which are presented in Fig. 5. For FM, the J_0's are exchange interactions within the single (Fe, Mn) sublattice involving all the exchange pairs of specified kind (e.g. Fe–Mn), whereas, for AF1, AF2 and AF3, the J_0''s are those between the two (Fe, Mn) sublattices. The exchange pairs are considered within the distance of 3a. The positive J_0 (J_0') indicates ferromagnetic coupling and the negative J_0 (J_0') means antiferromagnetic coupling. Since the single (Fe, Mn) sublattice of FM comprises the two (Fe, Mn) sublattices of AF1, AF2 and AF3, the J_0's of FM reflect the overall coupling while the J_0''s of AF1, AF2 and AF3 indicate the viability to form the specified antiferromagnetic state.

It is found in Fig. 5a that, the overall FM coupling can be stabilized for Fe–Fe, in contrast to the instability of FM alignment for Fe–Mn and Mn–Mn. When split into two magnetic sublattices (Fig. 5b–d), for AF2, the three types of interactions between sublattices turn to be weakly antiferromagnetically coupled when x increases, whereas, for AF1 and AF3, the interactions behave similarly to those presented in Fig. 5a. The J_0''s of AF1 and AF3 seem to dominate the corresponding J_0's in Fig. 5a. This is because the most significant exchange interactions happen between the nearest-neighbored atomic pairs in the (Fe,Mn) plane (not shown here) which are missed in the AF2 but are included in the AF1 and AF3 when calculating the J_0''s (cf. sublattices in Fig. 1). For AF2, the weak couplings between sublattices correspond to its relatively close stability to that of FM state. For AF1 and AF3, the antiferromagnetic J_0'(Fe–Mn) and J_0'(Mn–Mn) competes with the ferromagnetic J_0'(Fe–Fe). Therefore, at low Mn concentration, the ferromagnetic J_0'(Fe–Fe) is strong enough to keep the parallel alignment, although this results in unfavored parallel Fe–Mn alignment, accounting for the low energies of FM–(AF1/AF3) states as presented in Fig. 3. At moderate Mn concentration, AF1 becomes most stable because the ferromagnetic J_0'(Fe–Fe) is weaker (easier to be surmounted) in AF1 than in AF3. At high Mn concentration, the antiferromagnetic J_0(Mn–Mn) is very strong to form magnetic structure based on AF3.

4. Conclusion

To summarize, this study has calculated a series of possible magnetic configurations using EMTO-CPA method. The calculation shows that, on doping Mn, FM is no longer stable. The energies of different configurations are close to each other at $x=0.2$. For $0.22 < x < 0.75$, AF1 is stabilized. The analysis of their energetic stabilities in combination with the comparison between theoretical and experimental $\overline{\mu}_{(Fe,Mn)}$ suggests that $FM^{\uparrow}-FM^{\downarrow}$ is only stable in a narrow composition range of $x \le 0.06$, in contrast to the experimental results measured in the films, which showed that $FM^{\uparrow}-FM^{\downarrow}$ exists in a wide range of $x \le 0.5$ [9]. This study gives the most stable configuration of FM–AF3 around $x=0.8$, which was not reported in experiments. The sudden drop in the experimental $\overline{\mu}_{(Fe,Mn)}$ at $x=0.86$ is due to the existence of $AF3^{\uparrow}-AF3^{\downarrow}$ phase. The composition-dependent strength of magnetic couplings between sublattices in AF1, AF2 and AF3 dominates their stabilities.

Acknowledgments

The authors acknowledge the National Basic Research Program of China (973 program, Grant no. 2014CB643702), Preferentially Funded Postdoctoral Project of Zhejiang Province (BSH1402079), and NSFC under Grant nos. 51401227 and 51101168. H.B.L. acknowledges the assistances from Prof. Qing-Miao Hu and Dr. Song Lu.

References

[1] B.R. Bian, W.X. Xia, J. Du, J. Zhang, J.P. Liu, Z.H. Guo, A. Yan, Growth mechanisms and size control of FePt nanoparticles synthesized using $Fe(CO)_x$($x < 5$)–oleylamine and platinum(II) acetylacetonate, Nanoscale 5 (2013) 2454.

[2] J.-U. Thiele, L. Folks, M.F. Toney, D.K. Weller, Perpendicular magnetic anisotropy and magnetic domain structure in sputtered epitaxial FePt (001) $L1_0$ films, J. Appl. Phys. 84 (1998) 5686.

[3] T.J. Klemmer, N. Shukla, C. Liu, X.W. Wu, E.B. Svedberg, O. Mryasov, R. W. Chantrell, D. Weller, M. Tanase, D.E. Laughlin, Structural studies of $L1_0$ FePt nanoparticles, Appl. Phys. Lett. 81 (2002) 2220.

[4] C.-H. Lai, C.-H. Yang, C.C. Chiang, Ion-irradiation-induced direct ordering of $L1_0$ FePt phase, Appl. Phys. Lett. 83 (2003) 4550.
[5] J. Lyubina, I. Opahle, M. Richter, O. Gutfleisch, K.-H. Müller, L. Schultz, O. Isnard, Influence of composition and order on the magnetism of Fe–Pt alloys: neutron powder diffraction and theory, Appl. Phys. Lett. 89 (2006) 032506.
[6] R.V. Chepulskii, W.H. Butler, Ab initio magnetocrystalline anisotropy at nanoscale: the case of FePt, Appl. Phys. Lett. 100 (2012) 142405.
[7] T. Suzuki, H. Kanazawa, A. Sakuma, Magnetic and structural properties of quaternary $(Fe–Co–Ni)_{50}$ Pt_{50} alloy thin films, IEEE Trans. Magn. 38 (2002) 2794.
[8] T. Burkert, O. Eriksson, S.I. Simak, A.V. Ruban, B. Sanyal, L. Nordström, J. M. Wills, Magnetic anisotropy of $L1_0$ FePt and $Fe_{1-x}Mn_xPt$, Phys. Rev. B 71 (2005) 134411.
[9] G. Meyer, J.-U. Thiele, Effective electron-density dependence of the magnetocrystalline anisotropy in highly chemically ordered pseudobinary $(Fe_{1-x}Mn_x)_{50}Pt_{50}$ $L1_0$ alloys, Phys. Rev. B 73 (2006) 214438.
[10] D.C. Berry, K. Barmak, Effect of alloy composition on the thermodynamic and kinetic parameters of the $A1$ to $L1_0$ transformation in FePt FeNiPt and FeCuPt films, J. Appl. Phys. 102 (2007) 024912.
[11] M.E. Gruner, P. Entel, Structural and magnetic properties of ternary $Fe_{1-x}Mn_xPt$ nanoalloys from first principles, Beilstein J. Nanotechnol. 2 (2011) 162.
[12] B. Wang, K. Barmak, T.J. Klemmer, The $A1$ to $L1_0$ transformation in FePt films with ternary alloying additions of Mg, V, Mn, and B, J. Appl. Phys. 109 (2011) 07B739.
[13] D.B. Xu, J.S. Chen, T.J. Zhou, G.M. Chow, Effects of Mn doping on temperature-dependent magnetic properties of $L1_0$ FeMnPt, J. Appl. Phys. 109 (2011) 07B747.
[14] A.Z. Menshikov, V.P. Antropov, G.P. Gasnikova, Y.A. Dorofeyev, V.A. Kazantsev, Magnetic phase diagram of ordered $Fe_{1-x}Mn_xPt$ alloys, J. Magn. Magn. Mater. 65 (1987) 159.
[15] R.M. Dreizler, E.K.U. Gross, Density Functional Theory, Springer, Berlin, 1998.
[16] Z. Lu, R.V. Chepulskii, W.H. Butler, First-principles study of magnetic properties of $L1_0$-ordered MnPt and FePt alloys, Phys. Rev. B 81 (2010) 094437.
[17] P. Soven, Coherent-potential model of substitutional disordered alloys, Phys. Rev. 156 (1967) 809.
[18] B.L. Gyorffy, Coherent-potential approximation for a nonoverlapping-muffin-tin-potential model of random substitutional alloys, Phys. Rev. B 5 (1972) 2382.
[19] L. Vitos, Total-energy method based on the exact muffin-tin orbitals theory, Phys. Rev. B 64 (2001) 014107.
[20] L. Vitos, Computational Quantum Mechanics for Materials Engineers: The EMTO Method and Applications, Springer-Verlag, London, 2007.
[21] J.P. Perdew, K. Burke, M. Ernzerhof, Generalized gradient approximation made simple, Phys. Rev. Lett. 77 (1996) 3865.
[22] D.J. Chadi, M.L. Cohen, Special points in the Brillouin zone, Phys. Rev. B 8 (1973) 5747.
[23] A.I. Liechtenstein, M.I. Katsnelson, V.P. Antropov, V.A. Gubanov, Local spin density functional approach to the theory of exchange interactions in ferromagnetic metals and alloys, J. Magn. Magn. Mater. 67 (1987) 65.
[24] G. Brown, B. Kraczek, A. Janotti, T.C. Schulthess, G.M. Stocks, D.D. Johnson, Competition between ferromagnetism and antiferromagnetism in FePt, Phys. Rev. B 68 (2003) 052405.